

Effort: Efficient Orthogonal Modeling for Generalizable AI-Generated Image Detection

Zhiyuan Yan^{1,2*}, Jiangming Wang^{2*}, Zhendong Wang^{3*}, Peng Jin¹, Ke-Yue Zhang², Shen Chen²,
Taiping Yao², Shouhong Ding^{2†}, Baoyuan Wu⁴, Li Yuan^{1†}
School of Electronic and Computer Engineering, Peking University¹,
Tencent Youtu Lab², University of Science and Technology of China³,
School of Data Science, The Chinese University of Hong Kong, Shenzhen⁴

Abstract

Existing AI-generated image (AIGI) detection methods often suffer from limited generalization performance. In this paper, we identify a crucial yet previously overlooked **asymmetry phenomenon** in AIGI detection: during training, models tend to quickly overfit to specific fake patterns in the training set, while other information is not adequately captured, leading to poor generalization when faced with new fake methods. A key insight is to incorporate the rich semantic knowledge embedded within large-scale vision foundation models (VFMs) to expand the previous discriminative space (based on forgery patterns only), such that the discrimination is decided by both forgery and semantic cues, thereby reducing the overfitting to specific forgery patterns. A straightforward solution is to fully fine-tune VFMs, but it risks distorting the well-learned semantic knowledge, pushing the model back toward overfitting. To this end, we design a novel approach called **Effort**: **Efficient orthogonal modeling for generalizable AIGI detection**. Specifically, we employ Singular Value Decomposition (SVD) to construct the orthogonal semantic and forgery subspaces. By freezing the principal components and adapting the residual components ($\sim 0.19M$ parameters), we preserve the original semantic subspace and use its orthogonal subspace for learning forgeries. Extensive experiments on AIGI detection benchmarks demonstrate the superior effectiveness of our approach.

1. Introduction

The rapid development of AI generative technologies has significantly lowered the barrier for creating highly realistic fake images. As deep generative models advance and mature [21, 28, 68], the proliferation of AI-generated im-

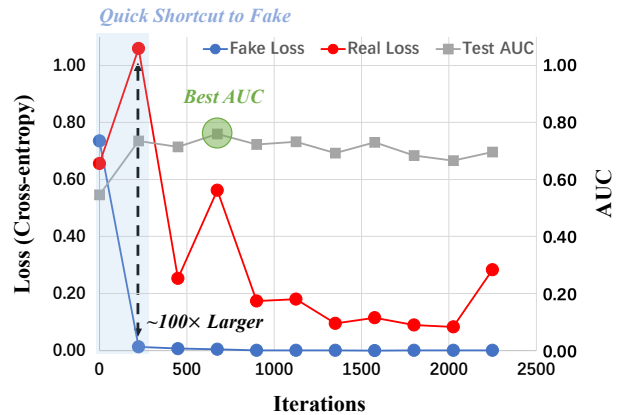


Figure 1. **Evidence for illustrating the asymmetry phenomenon in AI-generated image detection.** We show that the baseline detector (*i.e.*, Xception [70]) tends to **quickly overfit to the fake patterns** in the training set, causing the generalization issue when facing previously unseen fake methods.

ages (AIGIs) has drawn considerable attention, driven by their ability to produce high-quality content with relative ease. However, these advancements also introduce significant risks, if misused for malicious purposes such as deepfakes (mainly including face-swapping [39] and face-reenactment [81]), which may violate personal privacy, spread misinformation, and erode trust in digital media. Consequently, there is an urgent need to develop a reliable and robust framework for detecting AIGIs.¹

Most existing studies in AIGI detection [70, 86] typically approach the real/fake classification problem as a symmetric binary classification task, akin to the “cat versus dog” problem. A standard binary classifier, often based on deep neural networks, is trained to distinguish between real and fake images by predicting the likelihood of a given test im-

* Equal Contribution.

† Corresponding Author.

¹In the context of this research, AIGI primarily refers to deepfakes (face-swapping) and synthetic images (*e.g.*, nature or arts).

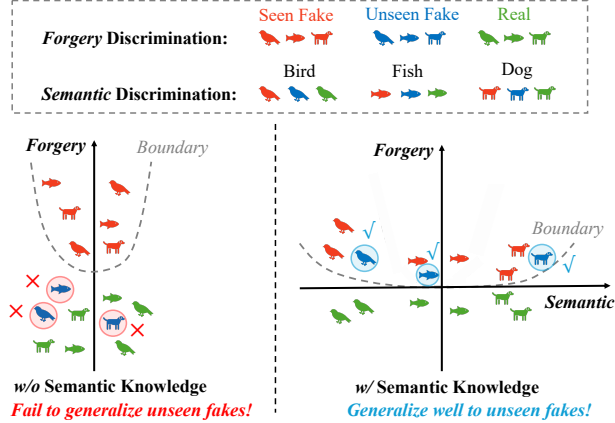


Figure 2. **Illustration of the comparison without and with incorporating semantic knowledge.** Naively trained models rely solely on forgery patterns for discrimination (the left), while incorporating semantic knowledge expands the discrimination space (the right), such that the discrimination is decided by both forgery and semantic cues, thereby alleviating the overfitting to seen fakes.

age being fake during inference. Although this paradigm yields promising results when the training and testing distributions (in terms of fake generation methods) are similar, its performance tends to degrade significantly when applied to previously unseen fake methods.

To understand the underlying reasons for the failure in generalization, we conducted extensive preliminary investigations and identified an *asymmetry phenomenon* in AIGI detection: naively trained models tend to take the shortcut and quickly overfit the specific fake patterns in the training set, resulting in the undesirable generalization performance when facing novel fake methods. Visualization in Fig. 1 corroborates this observation. Specifically, the vanilla detector (*i.e.*, Xception [70]) quickly fits the fake patterns at the very early training stage (only a few iterations), resulting in a very low loss of fake, while the real loss is significantly higher than the fake loss ($\sim 100\times$ larger). This is likely because existing AIGI detection datasets [70, 86] typically contain limited and homogeneous fake types, while real samples exhibit significantly greater diversity and variance (such as different categories and scenarios). This asymmetry causes the detection model to quickly overfit to the *seen* forgery patterns during training, limiting its generalization to detect *unseen* fakes.

To address this, a key insight is to incorporate the rich semantic knowledge embedded within the large-scale vision foundation models (VFMs) to expand the previous discriminative space (relying on forgery pattern only), such that the discrimination is decided by both forgery and semantic cues. We provide an illustration example in Fig. 2 for intuitively understanding the role of semantic knowledge. Specifically, naively trained models rely solely on

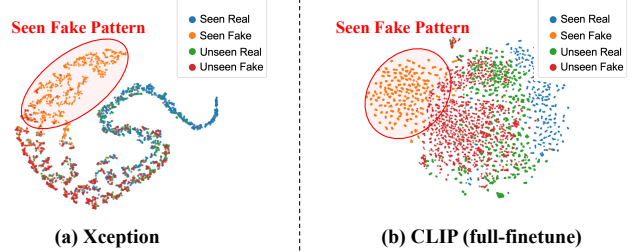


Figure 3. **t-SNE visualizations between Xception and CLIP (full-finetune).** We show that both models only learn the specific fake patterns within the training set, treating samples with seen fake patterns as fake while other samples are all considered real, thereby limiting their generalization in detecting unseen fakes.

forgery patterns for discrimination (the left), fitting well to the seen fakes but failing to generalize previously unseen fakes. When semantic knowledge is incorporated, the discrimination space is largely expanded, with different semantic categories such as Bird and Fish separated (the right). In this case, the discrimination is determined by both forgery and semantic cues, thus reducing the overfitting to the seen forgery patterns and enhancing the model’s generalization.

So, is naively fine-tuning a VFM sufficient to obtain a generalizable AIGI detector? Unfortunately, it risks distorting the well-learned semantic knowledge of the original VFM, pushing the VFM model back toward overfitting. The t-SNE results in Fig. 3 show that fully fine-tuning a VFM can still overfit the seen fake patterns, due to the mentioned asymmetry problem. Specifically, both the Xception (Vanilla CNN) and CLIP [65] (VFM) detector group only the specific fake patterns within the training set into a single cluster, while all other data, including real and fake from unseen manipulation methods are classified into the other cluster. This highlights that simply fine-tuning the VFMs (even using CLIP) is still insufficient to overcome the asymmetry issue and achieve robust generalization.

To this end, we design a novel approach called **Effort: Efficient orthogonal modeling for generalizable AIGI detection.** Specifically, we employ Singular Value Decomposition (SVD) to construct the orthogonal semantic and forgery subspaces. By freezing the principal components and adapting the residual components ($\sim 0.19M$ parameters), we preserve the original semantic subspace and use its orthogonal subspace for learning forgeries. We conduct experiments on both deepfake detection and synthetic image detection benchmarks and surprisingly find that our approach achieves significant superiority over other SOTAs with very few trainable parameters.

Overall, this work makes the following key contributions:

- **Asymmetry Phenomenon in AIGI Detection:** We intro-

duce the concept of asymmetry in AIGI detection, which has often been overlooked in previous works. A naively trained detector tends to quickly fit the seen fake methods well but, in doing so, it often overfits to specific fake patterns in the training set, limiting its generalization ability to detect unseen fake methods.

- **Semantic Knowledge Involved and Orthogonality:** We propose a novel approach, *Effort*, to address the asymmetry in AIGI detection by (1) leveraging the rich semantic knowledge within the Vision Foundation Models (VFM) to explain the previous discrimination space, alleviating the over-relying on forgery patterns only, and (2) Using SVD to construct the orthogonal semantic and forgery subspaces, avoiding the distortion of original well-learned semantic knowledge during learning fakes.
- **Striking Result and Efficiency:** *Effort* achieves remarkably high generalization performance on previously unseen forgeries using nearly only 0.19M tunable parameters, making it efficient and potentially scalable. Moreover, our approach can be applied to detect a broad range of AIGIs, including but not limited to face forgeries (*e.g.*, classical deepfakes) and synthetic natural images.

2. Related Work

Our work focuses on detecting AI-generated images (AIGIs), especially **deepfake images** (*e.g.*, face-swapping) and **synthetic images** (*e.g.*, nature or art), following [94]. As the majority of recent works specifically focus on dealing with the generalization issue, where the training and testing distribution differ (in terms of fake methods), we will briefly introduce the classical and recent detection methods toward generalization in deepfake and synthetic images, respectively.

Generalizable Deepfake Image Detection. The task of deepfake detection grapples profoundly with the issue of generalization. To tackle the generalization issue, one mainstream approach is *fake pattern learning*. Most existing works are within this line. These methods generally design a “transformation function”, *e.g.*, frequency transformation [42, 47, 53], blending operations [8, 44, 72, 99], reconstruction [4, 104], content/ID disentanglement [20, 30, 91], to transform the original input x into x' , where they believe that the more general fake patterns can be captured within the feature space of x' compared to x . However, given the ever-increasing diversity of forgery methods in the real world, it is unrealistic to elaborate all possible fake patterns and “expect” good generalization on unseen fake methods. Another notable direction is to *real distribution learning*, with a specific methodology involved: one-class anomaly detection [35, 40]. Specifically, [35] introduced a one-class-based anomaly detection, where “abnormal” data is detected by the proposed reconstruction error as the anomaly

score. [40] proposed a similar approach to create pseudo-fake “anomaly” samples by using image-level blending on different facial regions. However, it is challenging to ensure that the detector can learn a robust representation of real images by using the very limited real data in existing deepfake datasets (*e.g.*, the FF++ dataset [70] contains only 1,000 real videos with imbalanced facial attribute distributions [83]).

Generalizable Synthetic Image Detection. With the rapid advancement of existing AI generative technologies, the scope of forged content has expanded beyond facial forgeries to encompass a wide range of scenes. In this context, similar to the deepfake detection field, most existing works typically focus on *fake pattern learning* that mines the low-level forgery clues from different aspects. Specifically, several approaches have been proposed to capture low-level artifacts, including RGB data augmentations [86], frequency-based features [31], gradients [76], reconstruction artifacts [6, 54, 87], and neighboring pixel relationships [79], random-mapping feature [77]. To illustrate, BiHPF [31] amplifies artifact magnitudes through the application of dual high-pass filters, while LGrad [76] uses gradient information from pre-trained models as artifact representations. NPR [79] introduces a straightforward yet effective artifact representation by rethinking up-sampling operations. In addition to learning from scratch, there are also several research works [48, 61, 89] that perform *fake pattern learning* by leveraging the existing vision foundation models. For instance, UniFD [61] directly freezes the visual encoder of the pre-trained CLIP model and tunes only a linear layer for binary classification, demonstrating effective deepfake detection even with previously unseen sources. LASTED [89] proposes designing textual labels to supervise the CLIP vision model through image-text contrastive learning, advancing the field of synthetic image detection. These arts have shown notable improvement in generalization performance when facing previously unseen fake methods.

3. Methodology

3.1. Motivation

Detecting AI-generated images (AIGI) has become an increasingly important topic. Existing works typically formulate AIGI detection as a standard binary classification problem (just like “cat versus dog”) and often get unsatisfied generalization performance. Our preliminary investigation surprisingly found that the failure of generalization can be attributed to the previously overlooked *asymmetry phenomenon*, where a naive trained detector tends to quickly overfit the specific fake pattern present in the training set, thereby limiting its generalization when facing previously unseen fake methods. To better understand the reasons behind the failure generalization, we present **three important**

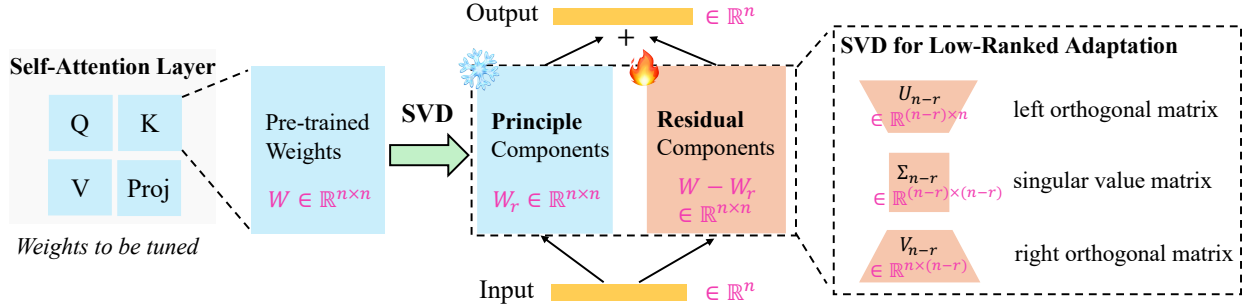


Figure 4. **The proposed SVD-based adaptation approach for AIGI detection.** The left branch is the decomposition matrix of the principle components approximation using SVD, while the right residual branch enables the orthogonal learning of real/fake discriminative features.

research questions (RQs) below.

RQ-1: Why do naively trained detectors fail to generalize to new unseen fake methods? In the previous sections, we have shown that the *asymmetry phenomenon*, where the naively trained models tend to quickly overfit the specific fake patterns in the training set, resulting in undesirable generalization performance when facing unseen fake methods (see Fig. 1). This is likely because existing AIGI detection datasets [70, 86] typically contain limited and homogeneous fake types, while real samples exhibit significantly greater diversity and variance. This asymmetry causes the detection model to quickly overfit to the specific and limited forgery methods during training, dominating the model’s discrimination space and shaping the whole space to be low-ranked (see Fig. 3(a)), thereby limiting its representational capacity and eventually hurting the generalization. We will provide a deeper analysis and evidence of this claim in Sec. 4.3.

RQ-2: Why incorporating semantic knowledge helps to alleviate the model’s overfitting? Given RQ-1, to address the asymmetric problem, a key insight is to leverage the rich semantic knowledge of VFMs to expand and enrich the low-ranked discrimination space (relying on forgery patterns only) to higher-ranked, encouraging the final discrimination based on both forgery patterns and semantic knowledge, thereby improving the alleviating the overfitting to the forgery patterns. Recall that there are numerous well-trained and generalizable vision foundation models (VFMs) available such as CLIP [65], SigLIP [96], and BEIT-v2 [63], which have already learned rich and robust semantic representation. Thus, leveraging the extensive semantic knowledge within VFMs presents a reasonable solution to expand the low-ranked discrimination space and reduce overfitting.

RQ-3: Why do naively fine-tuning VFMs fail to generalize to new unseen fake methods? A straightforward solution that incorporates semantic knowledge into detection is fine-tuning VFMs, but it risks distorting the well-learned seman-

tic knowledge, falling back to the overfitting to the forgery patterns, similar to a vanilla CNN baseline, as shown in Fig. 3. To overcome these issues, we propose to achieve the orthogonality of semantic and forgery subspaces, where the forgery pattern learning is conducted within a new subspace that is orthogonal to the original semantic subspace, avoiding the distortion of the pre-existing semantic knowledge. To achieve this, we introduce a novel approach that uses SVD to explicitly construct the orthogonal semantic and forgery subspaces by freezing the principal components for representing semantic knowledge, while adapting only the residual components for forgery pattern learning.

3.2. Effort Approach

The overall pipeline of the proposed *Effort* approach is illustrated in Fig. 4, aiming to address the asymmetry phenomena in AIGI detection. In general, our approach involves the Singular Value Decomposition (SVD) to construct explicit orthogonal semantic and forgery subspaces, avoiding the distortion of well-learned semantic knowledge during fake pattern learning.

Formally, given a pre-trained weight matrix $W \in \mathbb{R}^{d_1 \times d_2}$ for a certain linear layer, we perform SVD to decompose W :

$$W = U\Sigma V^\top, \quad (1)$$

where $U \in \mathbb{R}^{d_1 \times d_1}$ and $V \in \mathbb{R}^{d_2 \times d_2}$ are orthogonal matrices containing the left and right singular vectors, respectively, and $\Sigma \in \mathbb{R}^{d_1 \times d_2}$ is a diagonal matrix with singular values on the diagonal. Since the linear layer of VFM generally has the same input and output dimensions, we consider the case of SVD with $d_1 = d_2 = n$ in the following discussion.

To obtain a rank- r approximation of the pre-trained weight matrix, we retain only the top r singular values and corresponding singular vectors:

$$W \approx W_r = U_r \Sigma_r V_r^\top, \quad (2)$$

where $U_r \in \mathbb{R}^{n \times r}$, $\Sigma_r \in \mathbb{R}^{r \times r}$, and $V_r \in \mathbb{R}^{n \times r}$. We

keep W_r frozen during training to preserve the knowledge learned from real images.

The residual component, defined as the difference between the pre-trained weights and the SVD approximation, is used to learn representations specific to fake images:

$$\Delta W = W - W_r = U_{n-r} \Sigma_{n-r} V_{n-r}^\top, \quad (3)$$

where $U_{n-r} \in \mathbb{R}^{n \times (n-r)}$, $\Sigma_{n-r} \in \mathbb{R}^{(n-r) \times (n-r)}$, $V_{n-r} \in \mathbb{R}^{n \times (n-r)}$. It is important to note that ΔW represents a learnable form associated with the remaining singular value decomposition, reflecting slight modifications or perturbations to the original weight matrix.

During training, we only optimize ΔW while keeping U_r , Σ_r , and V_r fixed. This implementation ensures that the model retains its capability to process real images via the SVD approximation and adapts to detect deepfakes through the trivial residual components of the weight matrix.

To encourage the ΔW to capture both useful and meaningful discrepancy between the real and fake, it's significant to guarantee that optimizing ΔW does not change the properties of the overall weight matrix W (i.e., Minimize the impact on the real information of the pre-trained weight as much as possible). Thus, we proposed two constraints to realize this goal:

Orthogonal Constraint. We maintain the orthogonality among each singular vector to keep orthogonal subspace for learning real/fake:

$$\mathcal{L}_{\text{orth}} = \|\hat{U}^\top \hat{U} - I\|_F^2 + \|\hat{V}^\top \hat{V} - I\|_F^2, \quad (4)$$

where $\hat{U} \in \mathbb{R}^{n \times n}$ denote the concatenation of U_r and U_{n-r} along the row dimension, $\hat{V} \in \mathbb{R}^{n \times n}$ denote the concatenation of V_r and V_{n-r} along the row dimension, $\|\cdot\|_F$ denotes the Frobenius norm, and I is the identity matrix of appropriate dimensions.

Singular Value Constraint. The singular values can be interpreted as a type of scaling that affects the magnitude of the corresponding singular vectors. There is a relationship between singular values and the Frobenius norm of the weight matrix being decomposed:

$$\|W\|_F = \sqrt{\sum_i \sigma_i^2}, \quad (5)$$

where σ_i denotes the i -th singular value of the corresponding weight matrix.

To maximize the reduction of the impact of real knowledge, we constrain the singular values of the optimized weight matrix \hat{W} to remain consistent with those of the original weight matrix W :

$$\mathcal{L}_{\text{ksv}} = \left| \sum_{i=r+1}^n \hat{\sigma}_i^2 - \sum_{i=r+1}^n \sigma_i^2 \right| = \left| \|\hat{W}\|_F^2 - \|W\|_F^2 \right| \quad (6)$$

where \hat{W} represents the weights after the optimization of W , and $|\cdot|$ represents the absolute value. Note that this regularization will control the importance of the ΔW during optimization to prevent overfitting of learning real/fake.

Loss Function. The overall loss function for training the model combines the classification loss \mathcal{L}_{cls} (e.g., cross-entropy loss for binary classification) and the orthogonality regularization loss:

$$\mathcal{L} = \mathcal{L}_{\text{cls}} + \lambda_1 \frac{1}{m} \sum_i^m \mathcal{L}_{\text{orth}}^i + \lambda_2 \frac{1}{m} \sum_i^m \mathcal{L}_{\text{ksv}}^i, \quad (7)$$

where λ_1, λ_2 are hyperparameters that balance the importance of the corresponding regularization term, and m represents the number of pre-trained weight matrices on which our approach is applied.

In practice, we adapt our approach to the *linear layers* within the self-attention module across all transformer layers of the Vision Foundation Model (VFM) to leverage their rich, well-learned real distributions.

4. Experiment

4.1. Deepfake Image Detection

Implementation Details. We utilize CLIP ViT-L/14 [65] as the default vision foundation model (VFM). We also investigate other VFMs in Tab. 5. We follow the pre-processing and training pipeline and use the codebases of DeepfakeBench [92]. Additionally, we sample 8 frames from each video for training and 32 frames for inference, following [72]. We use the fixed learning rate of 2e-4 for training our approach and employ the Adam [36] for optimization. We set the batch size to 32 for both training and testing. We also employ several widely used data augmentations, such as Gaussian Blur and Image Compression, following other existing works [11, 72, 93]. For the evaluation metric, we report the widely-used video-level Area Under the Curve (AUC) to compare our approach with other works, following [46, 72, 90]. Similar to these works, we compute the average model's output probabilities of each video to obtain the video-level AUC.

Evaluation Protocols and Dataset. We adopt two widely used and standard protocols for evaluation: **Protocol-1:** cross-dataset evaluation and **Protocol-2:** cross-manipulation evaluation within the FF++ data domain. For **Protocol-1**, we conduct evaluations by training the models on FaceForensics++ (FF++) [70] and testing them on other seven deepfake detection datasets: Celeb-DF-v2 (CDF-v2) [45], DeepfakeDetection (DFD) [16], Deepfake Detection Challenge (DFDC) [15], the preview version of DFDC (DFDCP) [19], DeeperForensics (DFo) [32], WildDeepfake (WDF) [105], and FFIW [101]. Note that FF++ has three

Methods	Trainable Param.	Cross-dataset Evaluation							Cross-method Evaluation									
		CDF-v2	DFD	DFDC	DFDCP	DFo	WDF	FFIW	Avg.	UniFace	BleFace	MobSwap	e4s	FaceDan	FSGAN	InSwap	SimSwap	Avg.
F3Net [64]	22M	0.789	0.844	0.718	0.749	0.730	0.728	0.649	0.743	0.809	0.808	0.867	0.494	0.717	0.845	0.757	0.674	0.746
SPL [47]	21M	0.799	0.871	0.724	0.770	0.723	0.702	0.794	0.769	0.747	0.748	0.885	0.514	0.666	0.812	0.643	0.665	0.710
SRM [53]	55M	0.840	0.885	0.695	0.728	0.722	0.702	0.794	0.767	0.749	0.704	0.779	0.704	0.659	0.772	0.793	0.694	0.732
CORE [58]	22M	0.809	0.882	0.721	0.720	0.765	0.724	0.710	0.762	0.871	0.843	0.959	0.679	0.774	0.958	0.855	0.724	0.833
RECCE [4]	48M	0.823	0.891	0.696	0.734	0.784	0.756	0.711	0.779	0.898	0.832	0.925	0.683	0.848	0.949	0.848	0.768	0.844
SLADD [8]	21M	0.837	0.904	0.772	0.756	0.800	0.690	0.683	0.777	0.878	0.882	0.954	0.765	0.825	0.943	0.879	0.794	0.865
SBI [72]	18M	0.886	0.827	0.717	0.848	0.899	0.703	0.866	0.821	0.724	0.891	0.952	0.750	0.594	0.803	0.712	0.701	0.766
UCF [91]	47M	0.837	0.867	0.742	0.770	0.808	0.774	0.697	0.785	0.831	0.827	0.950	0.731	0.862	0.937	0.809	0.647	0.824
IID [30]	66M	0.838	0.939	0.700	0.689	0.808	0.666	0.762	0.789	0.839	0.789	0.888	0.766	0.844	0.927	0.789	0.644	0.811
TALL [90]	87M	0.831	0.833	0.693	0.739	0.793	0.673	0.679	0.749	0.714	0.699	0.805	0.651	0.768	0.863	0.762	0.616	0.735
LSDA† [94]	133M	0.875	0.881	0.701	0.812	0.768	0.797	0.724	0.794	0.872	0.875	0.930	0.694	0.721	0.939	0.855	0.793	0.835
ProDet† [11]	96M	0.926	0.901	0.707	0.828	0.879	0.781	0.751	0.828	0.908	0.929	0.975	0.771	0.747	0.928	0.837	0.844	0.867
CDFa† [46]	87M	0.938	0.954	0.830	0.881	0.973	0.796	0.777	0.878	0.762	0.756	0.823	0.631	0.803	0.942	0.772	0.757	0.781
Effort (Ours)	0.19M	0.956	0.965	0.843	0.909	0.977	0.848	0.921	0.917	0.962	0.873	0.953	0.983	0.926	0.957	0.936	0.926	0.940

Table 1. **Benchmarking Results of Cross-dataset Evaluations (Protocol-1) and Cross-method Evaluations (Protocol-2).** All detectors are trained on FF++_c23 [70] and evaluated on other fake data. The best results are highlighted in bold and the second is underlined. † indicates the results are obtained by using the model’s checkpoint provided by the authors, otherwise, the results are cited from [11, 92, 94].

Methods	GAN						Deep fakes	Low level		Perceptual loss		Guided	LDM			Glide			Dalle	mAP
	Pro-GAN	Cycle-GAN	Big-GAN	Style-GAN	Gau-GAN	Star-GAN		SITD	SAN	CRN	IMLE		200 steps	200 w/cfg	100 steps	100 27	50 27	100 10		
CNN-Spot [86]	100.0	93.47	84.50	99.54	89.49	98.15	89.02	73.75	59.47	98.24	98.40	73.72	70.62	71.00	70.54	80.65	84.91	82.07	70.59	83.58
Patchfor [5]	80.88	72.84	71.66	85.75	65.99	69.25	76.55	76.19	76.34	74.52	68.52	75.03	87.10	86.72	86.40	85.37	83.73	78.38	75.67	77.73
Co-occurrence [57]	99.74	80.95	50.61	98.63	53.11	67.99	59.14	68.98	60.42	73.06	87.21	70.20	91.21	89.02	92.39	89.32	88.35	82.79	80.96	78.11
Freq-spec [98]	55.39	100.0	75.08	55.11	66.08	100.0	45.18	47.46	57.12	53.61	50.98	57.72	77.72	77.25	76.47	68.58	64.58	61.92	67.77	66.21
F3Net† [64]	99.96	84.32	69.90	99.72	56.71	100.0	78.82	52.89	46.70	63.39	64.37	70.53	73.76	81.66	74.62	89.81	91.04	90.86	71.84	76.89
UniFD [61]	100.0	98.13	94.46	86.66	99.25	99.53	91.67	78.54	67.54	83.12	91.06	79.24	95.81	79.77	95.93	93.93	95.12	94.59	88.45	90.14
LGrad† [76]	100.0	93.98	90.69	99.86	79.36	99.98	67.91	59.42	51.42	63.52	69.61	87.06	99.03	99.16	99.18	93.23	95.10	94.93	97.23	86.35
FreqNet† [78]	99.92	99.63	96.05	99.89	99.71	98.63	99.92	94.42	74.59	80.10	75.70	96.27	96.06	100.0	62.34	99.80	99.78	96.39	77.78	91.95
NPR [79]	100.0	99.53	94.53	99.94	88.82	100.0	84.41	97.95	99.99	50.16	50.16	98.26	99.92	99.91	99.92	99.87	99.89	99.92	99.26	92.76
FatFormer† [48]	100.0	100.0	99.98	99.75	100.0	100.0	97.99	97.94	81.21	99.84	99.93	91.99	99.81	99.09	99.87	99.13	99.41	99.20	99.82	98.16
Effort (Ours)	100.0	100.0	99.99	99.77	100.0	100.0	98.95	97.53	97.53	100.0	100.0	95.39	99.99	99.89	100.0	99.87	99.92	99.98	99.96	99.41

Table 2. **Benchmarking Results of Cross-method Evaluations in terms of AP Performance on the UniversalFakeDetect Dataset.** † indicates that the results are obtained by using the official pre-trained model or reproduction.

Methods	GAN						Deep fakes	Low level		Perceptual loss		Guided	LDM			Glide			Dalle	mAcc
	Pro-GAN	Cycle-GAN	Big-GAN	Style-GAN	Gau-GAN	Star-GAN		SITD	SAN	CRN	IMLE		200 steps	200 w/cfg	100 steps	100 27	50 27	100 10		
CNN-Spot [86]	99.99	85.20	70.20	85.70	78.95	91.70	53.47	66.67	48.69	86.31	86.26	60.07	54.03	54.96	54.14	60.78	63.80	65.66	55.58	69.58
Patchfor [5]	75.03	68.97	68.47	79.16	64.23	63.94	75.54	75.14	75.28	72.33	55.30	67.41	76.50	76.10	75.77	74.81	73.28	68.52	67.91	71.24
Co-occurrence [57]	97.70	63.15	53.75	92.50	51.10	54.70	57.10	63.06	55.85	65.65	65.80	60.50	70.70	70.55	71.00	70.25	69.60	69.90	67.55	66.86
Freq-spec	49.90	99.90	50.50	49.90	50.30	99.70	50.10	50.00	48.00	50.60	50.10	50.90	50.40	50.40	50.30	51.70	51.40	50.40	50.00	55.45
F3Net† [64]	99.38	76.38	65.33	92.56	58.10	100.0	63.48	54.17	47.26	51.47	51.47	69.20	68.15	75.35	68.80	81.65	83.25	83.05	66.30	71.33
UniFD [61]	100.0	98.50	94.50	82.00	99.50	97.00	66.60	63.00	57.50	59.50	72.00	70.03	94.19	73.76	94.36	79.07	79.85	78.14	86.78	81.38
LGrad† [76]	99.84	85.39	82.88	94.83	72.45	99.62	58.00	62.50	50.00	50.74	50.78	77.50	94.20	95.85	94.80	87.40	90.70	89.55	88.35	80.28
FreqNet† [78]	97.90	95.84	90.45	97.55	90.24	93.41	97.40	88.92	59.04	71.92	67.35	86.70	84.55	99.58	65.56	85.69	97.40	88.15	59.06	85.09
NPR [79]	99.84	95.00	87.55	96.23	86.57	99.75	76.89	66.94	98.63	50.00	50.00	84.55	97.65	98.00	98.20	96.25	97.15	97.35	87.15	87.56
FatFormer† [48]	99.89	99.32	99.50	97.15	99.41	99.75	93.23	81.11	68.04	69.45	69.45	76.00	98.60	94.90	98.65	94.35	94.65	94.20	98.75	90.86
Effort (Ours)	100.0	99.85	99.60	95.05	99.60	100.0	87.60	92.50	81.50	98.90	98.90	69.15	99.30	96.80	99.45	97.45	97.80	97.15	98.05	95.19

Table 3. **Benchmarking Results of Cross-method Evaluations in terms of Acc Performance on the UniversalFakeDetect Dataset.** † indicates that the results are obtained by using the official pre-trained model or reproduction.

different compression versions and we adopt the c23 version for training all methods in our experiments, following most existing works [93]. For **Protocol-2**, we evaluate the models on the latest deepfake dataset DF40 [95], which contains the forgery data generated within the FF++ domain, ensuring the evaluation fake methods different but the data domain unchanged. In this manner, we can assess the model’s generalization when facing unseen fake methods, ignoring the impact of the data domain gap.

Evaluation Benchmarking. To provide a comprehensive benchmark for comparison, we introduce **13 competitive detectors**, including several classical detection methods such as F3Net [64] (ECCV’20), SPL [47] (CVPR’20),

SRM [47] (CVPR’21), CORE [58] (CVPRW’22), RECCE [4] (CVPR’22), and SBI [72] (CVPR’22), and also several latest SOTA methods (after 2023), such as UCF [91] (ICCV’23), IID [30] (CVPR’23), TALL [90] (ICCV’23), LSDA [94] (CVPR’24), ProDet [11] (NeurIPS’24), and CDFa [46] (ECCV’24). All detectors are trained on FF++ (c23) and tested on other fake data. Results in Tab. 1 demonstrate two notable advantages of our approach. **(1) generalizability:** we see that our approach consistently and largely outperforms other models across basically all tested scenarios, validating that our method is generalizable for detecting unseen fake data, even for the latest face-swapping techniques such as BleFace [73]. **(2) efficiency:** it is worth noting that our method only needs 0.19M

Table 4. **Ablation studies regarding the tunable $n - r$ values in SVD.** All models are trained on FF++ (c23) and tested on CDF-v2 and SimSwap. ‘‘FFT’’ indicates the full fine-tuning. ‘‘Linear-Prob’’ indicates fine-tuning the FC layer only.

Archs.		#Params	$n - r$	CDF-v2	SimSwap	Avg.
Baseline (Linear-Prob)		0.002M	–	0.765	0.769	0.767
Baseline (FFT)		307M	–	0.857	0.860	0.859
Ours	Variant-1	12M	64	0.946	0.935	0.941
	Variant-2	3M	16	0.948	0.930	0.939
	Variant-3	0.75M	4	0.955	0.921	0.938
	Variant-4	0.19M	1	0.956	0.926	0.941

Table 5. **Ablation studies regarding different vision foundation models (VFMs) were used.** All models are trained on FF++ (c23) and tested on CDF-v2 and SimSwap.

VFMs	#Params	#ImgSize	CDF-v2	SimSwap	Avg.
BEIT-v2 [63]	303M	224	0.855	0.821	0.838
+ Ours	0.14M	224	0.894	0.850	0.872
SigLIP [96]	316M	256	0.877	0.713	0.795
+ Ours	0.19M	256	0.895	0.778	0.867
CLIP [65]	307M	224	0.857	0.860	0.859
+ Ours	0.19M	224	0.956	0.926	0.941

parameters for training to achieve superior generalization. As we can see most latest SOTA detectors such as LSDA and ProDet all use about 100M parameters for training, while we are about **1,000× smaller**.

4.2. Synthetic Image Detection

Evaluation Metrics. We follow existing works [48, 61, 85] for benchmarking and report both average precision (AP) and classification accuracy (Acc). For Acc, we set the classification threshold for each dataset to 0.5 to ensure a fair comparison.

UniversalFakeDetect Datasets. We adhere to the protocol outlined in [61, 85] and utilize ProGAN’s real and fake images as our training dataset, which includes 20 subsets of generated images. The evaluation set contains 19 subsets derived from different kinds of generative models, including ProGAN [33], CycleGAN [102], BigGAN [2], StyleGAN [34], GauGAN [62], StarGAN [13], DeepFakes [69], SITD [7], SAN [14], CRN [10], IMLE [43], Guided (guided diffusion model)[17], LDM (latent diffusion model) [67], Glide [60], and DALLE [66].

Implementation Details. Similar to the setting of deepfake image detection, we adopt pre-trained CLIP ViT-L/14 as the backbone and use the Adam optimizer [36] with a fixed learning rate of $2e-4$. The batch size is set to 48. Other settings and details are the same with [61].

Evaluation Analysis. The AP and Acc results are presented in Tab. 2 and Tab. 3, respectively. Our method attains impressive detection results, achieving 95.19% mAcc and 99.41% mAP across the 19 test subsets. One similar approach to ours is UniFD, which also preserves the original semantic knowledge of CLIP and fine-tunes only the FC

Table 6. **Ablation studies regarding the singular value constraint (\mathcal{L}_{ksv}) and orthogonal constraint (\mathcal{L}_{orth}).** All models are trained on FF++ (c23) and tested on other datasets.

Ours			CDF-v2	DFDC	SimSwap	FSGAN	Avg.
SVD	\mathcal{L}_{ksv}	\mathcal{L}_{orth}					
×	×	×	0.857	0.758	0.860	0.939	0.854
✓	×	×	0.940	0.829	0.910	0.955	0.909
✓	✓	×	0.944	0.841	0.927	0.953	0.916
✓	×	✓	0.945	0.847	0.914	0.950	0.914
✓	✓	✓	0.956	0.843	0.926	0.957	0.921

layer for discrimination. In contrast to UniFD which performs discrimination in the semantic space, our approach utilizes SVD to create an orthogonal low-ranked subspace for learning forgeries while preserving the essential high-ranked semantic space, achieving the discrimination by leveraging both semantic and forgery subspaces, achieving a significant improvement of 9.27% in mAcc and 13.81% in mAP over UniFD. Besides, when compared to the SoTA method, FatFormer, we achieve 4.33% mAcc improvement without relying on the extra text encoder of CLIP. This further demonstrates the superiority of our approach.

4.3. Ablation Study and Analysis

How many singular values should be tuned when applying SVD? When applying SVD, we create the semantic (frozen) and forgery (tuning) subspaces. But a crucial question arises: how many singular values should be set aside for freezing and how many for tuning? To figure out the optimal empirical values for this, we carry out an ablation study. The purpose of this study is to evaluate the effectiveness of different values of $n - r$. Here, n represents the full-ranked dimension of the original weights, while r is the low-ranked dimension that we intend to tune. We examine four different variants with specific values for $n - r$, namely 64, 16, 6, and 1. Additionally, we include the baseline case, which is the full-finetune CLIP, for the sake of comparison. Results in Tab. 4 suggest that our approach largely outperforms the baseline. Moreover, the performance levels of the four variants are quite similar. This implies that none of these variants holds a distinct advantage when it comes to generalization. However, among them, variant-4 has the fewest trainable parameters. Consequently, we select this particular setting as the default option in our other experiments.

Compatibility with other vision foundation models. By default, we choose CLIP as the vision foundation model (VFM) in our experiments. To validate the generality and versatility of our approach, we conduct an ablation study to apply our method to other VFMs, including BEIT-v2 [63] and SigLIP [96]. Results in Tab. 5 show that our approach can be seamlessly applied to other existing VFMs for improving the model’s generalization performance.

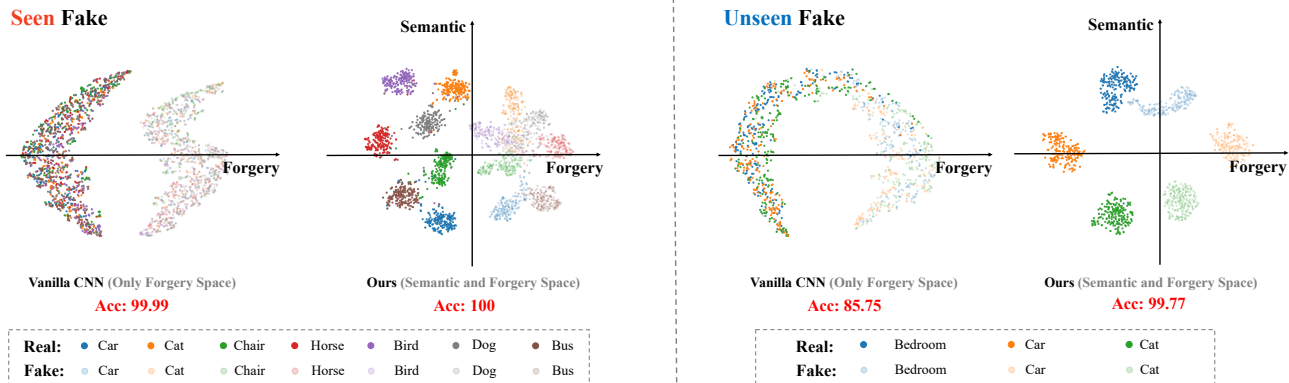


Figure 5. Evidence for verifying the illustration of Fig. 2, showing the latent distributions of vanilla CNN (e.g., Res50 [86]) and ours.

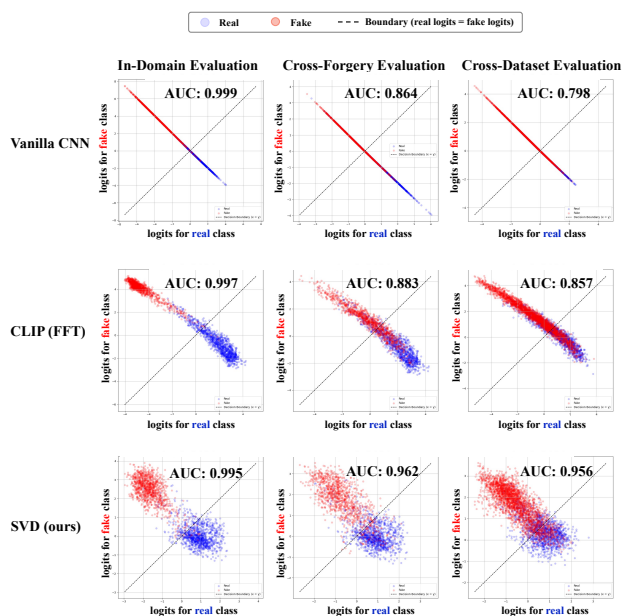


Figure 6. Evidence for validating the discrimination dimension from the logits space. Please refer to the text for details.

How to verify the naively trained models use only forgery patterns for discrimination? In our motivation (RQ-2), we argue that the naively trained models rely solely on forgery patterns for discrimination, as the models tend to overfit the seen fake patterns during training (see Fig. 1, Fig. 3, Fig. 5). To verify that the baseline models (a vanilla CNN, *i.e.*, Xception) indeed leverages only the forgery patterns for discrimination, we conduct a new visualization in Fig. 6, providing reasonable evidence to see the model’s discrimination behavior. Specifically, we visualize the model’s output, *i.e.*, logits, for both real and fake classes, and a dotted line for the boundary (to those samples with real logits equal to fake logits). As shown in Fig. 6, we see that all

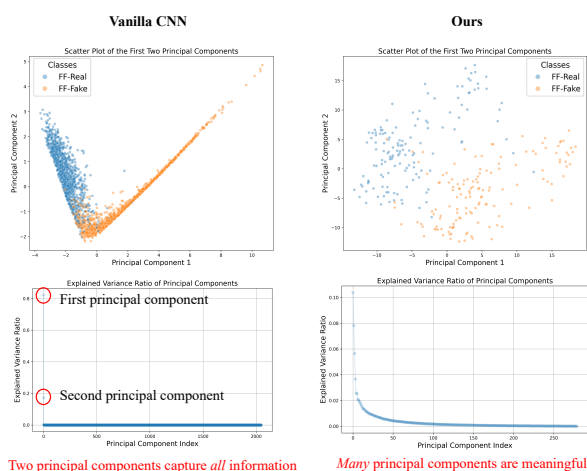


Figure 7. Evidence for validating the discrimination dimension from the feature space. We use PCA to analyze the rank of the feature space. Please refer to the text for details.

prediction samples of Xception lie in a linear line (similar to $y = -x + b$), indicating that the Xception relies on one dimension for discriminating real and fake. In addition, the CLIP contains rich semantic knowledge, but fully fine-tuning CLIP can distort the well-learned semantic knowledge, making it near to a line ($y = -x + b$). Finally, our approach maximizes the retention of semantic knowledge. We achieve this by learning forgeries within a new orthogonal subspace relative to the semantic subspaces, achieving superior generalization than the other two models.

Low-ranked feature space causes the model’s overfitting. We use Principal Component Analysis (PCA) to visualize the feature space with the two most principal components (the top row) and demonstrate the explained variance ratio of different principal components (the below row), which is similar to “how much of the total information

of the data is captured by each principal component”. Results in Fig. 7 show that the feature space of the Xception is highly low-ranked, with only two principal components to capture all information, resulting in limited generalization.

5. Conclusion

In this paper, we provide a new perspective to explain the failure reason of the generalization in AIGI detection, namely the asymmetry phenomena, where a naively trained detector very quickly shortcuts to the seen fake patterns, dominating the whole feature space and shaping it to be highly low-ranked, thereby limiting its expressivity and generalization. The key idea of this paper is to incorporate the rich semantic knowledge within the vision foundation models (VFMs) to expand the discrimination and feature space to higher-ranked, alleviating the model’s overfitting to seen fake patterns. A straightforward strategy is to directly fine-tune the VFM, but it risks distorting the learned semantic space, pushing the model back toward overfitting. To this end, we propose to decompose the original semantic space into two orthogonal subspaces for preserving semantic knowledge while learning forgery. We conduct extensive experiments on both deepfake and synthetic image detection benchmarks, showing the superior advantages in both generalization and efficiency.

References

- [1] Wukong, 2022. 5. In <https://xihe.mindspore.cn/modelzoo/wukong>, 2022. 5.
- [2] Andrew Brock, Jeff Donahue, and Karen Simonyan. Large scale gan training for high fidelity natural image synthesis. *arXiv*, 2018.
- [3] Andrew Brock et al. Large scale gan training for high fidelity natural image synthesis. In *International Conference on Learning Representations*, 2018.
- [4] Junyi Cao, Chao Ma, Taiping Yao, Shen Chen, Shouhong Ding, and Xiaokang Yang. End-to-end reconstruction-classification learning for face forgery detection. In *Proceedings of the IEEE/CVF Conference on Computer Vision and Pattern Recognition*, pages 4113–4122, 2022.
- [5] Lucy Chai, David Bau, Ser-Nam Lim, and Phillip Isola. What makes fake images detectable? understanding properties that generalize. In *Computer Vision—ECCV 2020: 16th European Conference, Glasgow, UK, August 23–28, 2020, Proceedings, Part XXVI 16*, pages 103–120. Springer, 2020.
- [6] Baoying Chen, Jishen Zeng, Jianquan Yang, and Rui Yang. Drcr: Diffusion reconstruction contrastive training towards universal detection of diffusion generated images. In *International Conference on Machine Learning*, 2024.
- [7] Chen Chen, Qifeng Chen, Jia Xu, and Vladlen Koltun. Learning to see in the dark. In *CVPR*, 2018.
- [8] Liang Chen, Yong Zhang, Yibing Song, Lingqiao Liu, and Jue Wang. Self-supervised learning of adversarial example: Towards good generalizations for deepfake detection. In *Proceedings of the IEEE/CVF Conference on Computer Vision and Pattern Recognition*, pages 18710–18719, 2022.
- [9] Liang Chen, Yong Zhang, Yibing Song, Jue Wang, and Lingqiao Liu. Ost: Improving generalization of deepfake detection via one-shot test-time training. In *Nips*, 2022.
- [10] Qifeng Chen and Vladlen Koltun. Photographic image synthesis with cascaded refinement networks. In *ICCV*, 2017.
- [11] Jikang Cheng, Zhiyuan Yan, Ying Zhang, Yuhao Luo, Zhongyuan Wang, and Chen Li. Can we leave deepfake data behind in training deepfake detector? *arXiv preprint arXiv:2408.17052*, 2024.
- [12] Jongwook Choi, Taehoon Kim, Yonghyun Jeong, Seungryul Baek, and Jongwon Choi. Exploiting style latent flows for generalizing deepfake video detection. In *Proceedings of the IEEE/CVF Conference on Computer Vision and Pattern Recognition*, pages 1133–1143, 2024.
- [13] Yunjey Choi, Minje Choi, Munyoung Kim, Jung-Woo Ha, Sunghun Kim, and Jaegul Choo. Stargan: Unified generative adversarial networks for multi-domain image-to-image translation. In *CVPR*, 2018.
- [14] Tao Dai, Jianrui Cai, Yongbing Zhang, Shu-Tao Xia, and Zhang Lei. Second-order attention network for single image super-resolution. In *CVPR*, 2019.
- [15] Deepfake detection challenge., 2020. <https://www.kaggle.com/c/deepfake-detection-challenge> Accessed 2021-04-24.
- [16] DFD., 2020. <https://ai.googleblog.com/2019/09/contributing-data-to-deepfake-detection.html> Accessed 2021-04-24.
- [17] Prafulla Dhariwal and Alex Nichol. Diffusion models beat gans on image synthesis. In *NeurIPS*, 2021.
- [18] Prafulla Dhariwal et al. Diffusion models beat gans on image synthesis. *Advances in Neural Information Processing Systems*, 34:8780–8794, 2021.
- [19] Brian Dolhansky, Russ Howes, Ben Pfau, Nicole Baram, and Cristian Canton Ferrer. The deepfake detection challenge (dfdc) preview dataset. *arXiv preprint arXiv:1910.08854*, 2019.
- [20] Shichao Dong, Jin Wang, Renhe Ji, Jiajun Liang, Haoqiang Fan, and Zheng Ge. Implicit identity leakage: The stumbling block to improving deepfake detection generalization. In *Proceedings of the IEEE/CVF Conference on Computer Vision and Pattern Recognition*, pages 3994–4004, 2023.
- [21] Ian Goodfellow, Jean Pouget-Abadie, Mehdi Mirza, Bing Xu, David Warde-Farley, Sherjil Ozair, Aaron Courville, and Yoshua Bengio. Generative adversarial networks. *Communications of the ACM*, 63(11):139–144, 2020.
- [22] Shuyang Gu, Dong Chen, Jianmin Bao, Fang Wen, Bo Zhang, Dongdong Chen, Lu Yuan, and Baining Guo. Vector quantized diffusion model for text-to-image synthesis. In *Proceedings of the IEEE/CVF Conference on Computer Vision and Pattern Recognition*, pages 10696–10706, 2022.
- [23] Zhihao Gu, Taiping Yao, Yang Chen, Shouhong Ding, and Lizhuang Ma. Hierarchical contrastive inconsistency learning for deepfake video detection. In *Proceedings of the European Conference on Computer Vision*, pages 596–613. Springer, 2022.

- [24] Jiazhi Guan, Hang Zhou, Zhibin Hong, Errui Ding, Jingdong Wang, Chengbin Quan, and Youjian Zhao. Delving into sequential patches for deepfake detection. *Advances in Neural Information Processing Systems*, 35:4517–4530, 2022.
- [25] Alexandros Haliassos, Konstantinos Vougioukas, Stavros Petridis, and Maja Pantic. Lips don't lie: A generalisable and robust approach to face forgery detection. In *CVPR*, 2021.
- [26] Alexandros Haliassos, Rodrigo Mira, Stavros Petridis, and Maja Pantic. Leveraging real talking faces via self-supervision for robust forgery detection. In *Proceedings of the IEEE/CVF Conference on Computer Vision and Pattern Recognition*, pages 14950–14962, 2022.
- [27] Kaiming He, Xiangyu Zhang, Shaoqing Ren, and Jian Sun. Deep residual learning for image recognition. In *Proceedings of the IEEE/CVF Conference on Computer Vision and Pattern Recognition*, pages 770–778, 2016.
- [28] Jonathan Ho, Ajay Jain, and Pieter Abbeel. Denoising diffusion probabilistic models. *Advances in neural information processing systems*, 33:6840–6851, 2020.
- [29] Edward J Hu, Yelong Shen, Phillip Wallis, Zeyuan Allen-Zhu, Yuanzhi Li, Shean Wang, Lu Wang, and Weizhu Chen. Lora: Low-rank adaptation of large language models. *arXiv preprint arXiv:2106.09685*, 2021.
- [30] Baojin Huang, Zhongyuan Wang, Jifan Yang, Jiabin Ai, Qin Zou, Qian Wang, and Dengpan Ye. Implicit identity driven deepfake face swapping detection. In *Proceedings of the IEEE/CVF conference on computer vision and pattern recognition*, pages 4490–4499, 2023.
- [31] Yonghyun Jeong et al. Bihpf: Bilateral high-pass filters for robust deepfake detection. In *Proceedings of the IEEE/CVF Winter Conference on Applications of Computer Vision*, pages 48–57, 2022.
- [32] Liming Jiang, Ren Li, Wayne Wu, Chen Qian, and Chen Change Loy. Deepforensics-1.0: A large-scale dataset for real-world face forgery detection. In *Proceedings of the IEEE/CVF Conference on Computer Vision and Pattern Recognition*, 2020.
- [33] Terro Karras, Timo Aila, Samuli Laine, and Jaakko Lehtinen. Progressive growing of gans for improved quality, stability, and variation. In *ICLR*, 2018.
- [34] Terro Karras, Samuli Laine, and Timo Aila. A style-based generator architecture for generative adversarial networks. In *CVPR*, 2019.
- [35] Hasam Khalid and Simon S Woo. Oc-fakedect: Classifying deepfakes using one-class variational autoencoder. In *Proceedings of the IEEE/CVF conference on computer vision and pattern recognition workshops*, pages 656–657, 2020.
- [36] Diederik P Kingma and Jimmy Ba. Adam: A method for stochastic optimization. *arXiv preprint arXiv:1412.6980*, 2014.
- [37] Chenqi Kong, Haoliang Li, and Shiqi Wang. Enhancing general face forgery detection via vision transformer with low-rank adaptation. In *2023 IEEE 6th International Conference on Multimedia Information Processing and Retrieval*, pages 102–107. IEEE, 2023.
- [38] Chenqi Kong, Anwei Luo, Peijun Bao, Yi Yu, Haoliang Li, Zengwei Zheng, Shiqi Wang, and Alex C Kot. Moe-ffd: Mixture of experts for generalized and parameter-efficient face forgery detection. *arXiv preprint arXiv:2404.08452*, 2024.
- [39] Pavel Korshunov and Sébastien Marcel. Deepfakes: a new threat to face recognition? assessment and detection. *arXiv preprint arXiv:1812.08685*, 2018.
- [40] Nicolas Larue, Ngoc-Son Vu, Vitomir Struc, Peter Peer, and Vassilis Christophides. Seeable: Soft discrepancies and bounded contrastive learning for exposing deepfakes. In *Proceedings of the IEEE/CVF International Conference on Computer Vision*, pages 21011–21021, 2023.
- [41] Da Li, Yongxin Yang, Yi-Zhe Song, and Timothy Hospedales. Learning to generalize: Meta-learning for domain generalization. In *Proceedings of the AAAI conference on artificial intelligence*, 2018.
- [42] Jiaming Li, Hongtao Xie, Jiahong Li, Zhongyuan Wang, and Yongdong Zhang. Frequency-aware discriminative feature learning supervised by single-center loss for face forgery detection. In *CVPR*, 2021.
- [43] Ke Li, Tianhao Zhang, and Jitendra Malik. Diverse image synthesis from semantic layouts via conditional imle. In *ICCV*, 2019.
- [44] Lingzhi Li, Jianmin Bao, Ting Zhang, Hao Yang, Dong Chen, Fang Wen, and Baining Guo. Face x-ray for more general face forgery detection. In *Proceedings of the IEEE/CVF Conference on Computer Vision and Pattern Recognition*, 2020.
- [45] Yuezun Li, Xin Yang, Pu Sun, Honggang Qi, and Siwei Lyu. Celeb-df: A new dataset for deepfake forensics. In *Proceedings of the IEEE/CVF Conference on Computer Vision and Pattern Recognition*, 2020.
- [46] Yuzhen Lin, Wentang Song, Bin Li, Yuezun Li, Jiangqun Ni, Han Chen, and Qiushi Li. Fake it till you make it: Curricular dynamic forgery augmentations towards general deepfake detection. *arXiv preprint arXiv:2409.14444*, 2024.
- [47] Honggu Liu, Xiaodan Li, Wenbo Zhou, Yuefeng Chen, Yuan He, Hui Xue, Weiming Zhang, and Nenghai Yu. Spatial-phase shallow learning: rethinking face forgery detection in frequency domain. In *Proceedings of the IEEE/CVF Conference on Computer Vision and Pattern Recognition*, 2021.
- [48] Huan Liu, Zichang Tan, Chuangchuang Tan, Yunchao Wei, Jingdong Wang, and Yao Zhao. Forgery-aware adaptive transformer for generalizable synthetic image detection. In *Proceedings of the IEEE/CVF Conference on Computer Vision and Pattern Recognition*, pages 10770–10780, 2024.
- [49] Ze Liu, Yutong Lin, Yue Cao, Han Hu, Yixuan Wei, Zheng Zhang, Stephen Lin, and Baining Guo. Swin transformer: Hierarchical vision transformer using shifted windows. In *Proceedings of the IEEE/CVF International Conference on Computer Vision*, pages 10012–10022, 2021.
- [50] Zhengzhe Liu et al. Global texture enhancement for fake face detection in the wild. In *Proceedings of the IEEE/CVF Conference on Computer Vision and Pattern Recognition*, pages 8060–8069, 2020.

- [51] Anwei Luo, Rizhao Cai, Chenqi Kong, Xiangui Kang, Jiwu Huang, and Alex C Kot. Forgery-aware adaptive vision transformer for face forgery detection. *arXiv preprint arXiv:2309.11092*, 2023.
- [52] Anwei Luo, Chenqi Kong, Jiwu Huang, Yongjian Hu, Xiangui Kang, and Alex C Kot. Beyond the prior forgery knowledge: Mining critical clues for general face forgery detection. *IEEE Transactions on Information Forensics and Security*, 19:1168–1182, 2023.
- [53] Yuchen Luo, Yong Zhang, Junchi Yan, and Wei Liu. Generalizing face forgery detection with high-frequency features. In *Proceedings of the IEEE/CVF Conference on Computer Vision and Pattern Recognition*, 2021.
- [54] Yunpeng Luo, Junlong Du, Ke Yan, and Shouhong Ding. Lare²: Latent reconstruction error based method for diffusion-generated image detection. In *Proceedings of the IEEE/CVF Conference on Computer Vision and Pattern Recognition*, pages 17006–17015, 2024.
- [55] Changtao Miao, Zichang Tan, Qi Chu, Huan Liu, Honggang Hu, and Nenghai Yu. F 2 trans: High-frequency fine-grained transformer for face forgery detection. *IEEE Transactions on Information Forensics and Security*, 18:1039–1051, 2023.
- [56] MidJourney. <https://www.midjourney.com/home>.
- [57] Lakshmanan Nataraj, Tajuddin Manhar Mohammed, Shivkumar Chandrasekaran, Arjuna Flenner, Jawadul H Bappy, Amit K Roy-Chowdhury, and BS Manjunath. Detecting gan generated fake images using co-occurrence matrices. *arXiv preprint arXiv:1903.06836*, 2019.
- [58] Yunsheng Ni, Depu Meng, Changqian Yu, Chengbin Quan, Dongchun Ren, and Youjian Zhao. Core: Consistent representation learning for face forgery detection. In *Proceedings of the IEEE/CVF Conference on Computer Vision and Pattern Recognition Workshop*, pages 12–21, 2022.
- [59] Alex Nichol, Prafulla Dhariwal, Aditya Ramesh, Pranav Shyam, Pamela Mishkin, Bob McGrew, Ilya Sutskever, and Mark Chen. Glide: Towards photorealistic image generation and editing with text-guided diffusion models. *arXiv preprint arXiv:2112.10741*, 2021.
- [60] Alex Nichol, Prafulla Dhariwal, Aditya Ramesh, Pranav Shyam, Pamela Mishkin, Bob McGrew, Ilya Sutskever, and Mark Chen. Glide: Towards photorealistic image generation and editing with text-guided diffusion models. In *ICML*, 2022.
- [61] Utkarsh Ojha et al. Towards universal fake image detectors that generalize across generative models. In *Proceedings of the IEEE/CVF Conference on Computer Vision and Pattern Recognition*, pages 24480–24489, 2023.
- [62] Taesung Park, Ming-Yu Liu, Ting-Chun Wang, and Jun-Yan Zhu. Semantic image synthesis with spatially-adaptive normalization. In *Proceedings of the IEEE Conference on Computer Vision and Pattern Recognition*, 2019.
- [63] Zhiliang Peng, Li Dong, Hangbo Bao, Qixiang Ye, and Furu Wei. Beit v2: Masked image modeling with vector-quantized visual tokenizers. *arXiv preprint arXiv:2208.06366*, 2022.
- [64] Yuyang Qian, Guojun Yin, Lu Sheng, Zixuan Chen, and Jing Shao. Thinking in frequency: Face forgery detection by mining frequency-aware clues. In *European Conference Computer Vision*, pages 86–103. Springer, 2020.
- [65] Alec Radford, Jong Wook Kim, Chris Hallacy, Aditya Ramesh, Gabriel Goh, Sandhini Agarwal, Girish Sastry, Amanda Askell, Pamela Mishkin, Jack Clark, et al. Learning transferable visual models from natural language supervision. In *International conference on machine learning*, pages 8748–8763. PMLR, 2021.
- [66] Aditya Ramesh, Mikhail Pavlov, Gabriel Goh, Scott Gray, Chelsea Voss, Alec Radford, Mark Chen, and Ilya Sutskever. Zero-shot text-to-image generation. In *ICML*, 2021.
- [67] Robin Rombach, Andreas Blattmann, Dominik Lorenz, Patrick Esser, and Bjorn Ommer. High-resolution image synthesis with latent diffusion models. In *CVPR*, 2022.
- [68] Robin Rombach, Andreas Blattmann, Dominik Lorenz, Patrick Esser, and Björn Ommer. High-resolution image synthesis with latent diffusion models. In *Proceedings of the IEEE/CVF conference on computer vision and pattern recognition*, pages 10684–10695, 2022.
- [69] Andreas Rössler, Davide Cozzolino, Luisa Verdoliva, Christian Riess, Justus Thies, and Matthias Nießner. FaceForensics++: Learning to detect manipulated facial images. In *International Conference on Computer Vision*, 2019.
- [70] Andreas Rössler, Davide Cozzolino, Luisa Verdoliva, Christian Riess, Justus Thies, and Matthias Nießner. FaceForensics++: Learning to detect manipulated facial images. In *Proceedings of the IEEE/CVF Conference on International Conference on Computer Vision*, pages 1–11, 2019.
- [71] Rui Shao, Tianxing Wu, Liqiang Nie, and Ziwei Liu. Deepfake-adapter: Dual-level adapter for deepfake detection. *arXiv preprint arXiv:2306.00863*, 2023.
- [72] Kaede Shiohara and Toshihiko Yamasaki. Detecting deepfakes with self-blended images. In *Proceedings of the IEEE/CVF Conference on Computer Vision and Pattern Recognition*, pages 18720–18729, 2022.
- [73] Kaede Shiohara, Xingchao Yang, and Takafumi Takeuchi. Blendface: Re-designing identity encoders for face-swapping. In *Proceedings of the IEEE/CVF International Conference on Computer Vision*, pages 7634–7644, 2023.
- [74] Ke Sun, Hong Liu, Qixiang Ye, Yue Gao, Jianzhuang Liu, Ling Shao, and Rongrong Ji. Domain general face forgery detection by learning to weight. In *Proceedings of the AAAI conference on Artificial Intelligence*, pages 2638–2646, 2021.
- [75] Ke Sun, Taiping Yao, Shen Chen, Shouhong Ding, Jilin Li, and Rongrong Ji. Dual contrastive learning for general face forgery detection. In *Proceedings of the AAAI Conference on Artificial Intelligence*, pages 2316–2324, 2022.
- [76] Chuangchuang Tan, Yao Zhao, Shikui Wei, Guanghua Gu, and Yunchao Wei. Learning on gradients: Generalized artifacts representation for gan-generated images detection. In *Proceedings of the IEEE/CVF Conference on Computer Vision and Pattern Recognition (CVPR)*, pages 12105–12114, 2023.

- [77] Chuangchuang Tan, Ping Liu, RenShuai Tao, Huan Liu, Yao Zhao, Baoyuan Wu, and Yunchao Wei. Data-independent operator: A training-free artifact representation extractor for generalizable deepfake detection. *arXiv preprint arXiv:2403.06803*, 2024.
- [78] Chuangchuang Tan, Yao Zhao, Shikui Wei, Guanghua Gu, Ping Liu, and Yunchao Wei. Frequency-aware deepfake detection: Improving generalizability through frequency space domain learning. In *Proceedings of the AAAI Conference on Artificial Intelligence*, pages 5052–5060, 2024.
- [79] Chuangchuang Tan, Yao Zhao, Shikui Wei, Guanghua Gu, Ping Liu, and Yunchao Wei. Rethinking the up-sampling operations in cnn-based generative network for generalizable deepfake detection. In *Proceedings of the IEEE/CVF Conference on Computer Vision and Pattern Recognition*, pages 28130–28139, 2024.
- [80] Mingxing Tan and Quoc Le. Efficientnet: Rethinking model scaling for convolutional neural networks. In *International Conference on Machine Learning*, pages 6105–6114. PMLR, 2019.
- [81] Justus Thies, Michael Zollhofer, Marc Stamminger, Christian Theobalt, and Matthias Nießner. Face2face: Real-time face capture and reenactment of rgb videos. In *Proceedings of the IEEE/CVF Conference on Computer Vision and Pattern Recognition*, 2016.
- [82] Hugo Touvron, Matthieu Cord, Matthijs Douze, Francisco Massa, Alexandre Sablayrolles, and Hervé Jégou. Training data-efficient image transformers & distillation through attention. In *International Conference on Machine Learning*, pages 10347–10357. PMLR, 2021.
- [83] Loc Trinh and Yan Liu. An examination of fairness of ai models for deepfake detection. *arXiv preprint arXiv:2105.00558*, 2021.
- [84] Junke Wang, Zuxuan Wu, Wenhao Ouyang, Xintong Han, Jingjing Chen, Yu-Gang Jiang, and Ser-Nam Li. M2tr: Multi-modal multi-scale transformers for deepfake detection. In *Proceedings of the 2022 International Conference on Multimedia Retrieval*, pages 615–623, 2022.
- [85] Sheng-Yu Wang, Oliver Wang, Richard Zhang, Andrew Owens, and Alexei A Efros. Cnn-generated images are surprisingly easy to spot...for now. In *CVPR*, 2020.
- [86] Sheng-Yu Wang, Oliver Wang, Richard Zhang, Andrew Owens, and Alexei A Efros. Cnn-generated images are surprisingly easy to spot... for now. In *Proceedings of the IEEE/CVF Conference on Computer Vision and Pattern Recognition*, pages 8695–8704, 2020.
- [87] Zhendong Wang, Jianmin Bao, Wengang Zhou, Weilun Wang, Hezhen Hu, Hong Chen, and Houqiang Li. Dire for diffusion-generated image detection. In *Proceedings of the IEEE/CVF International Conference on Computer Vision*, pages 22445–22455, 2023.
- [88] Zhendong Wang, Jianmin Bao, Wengang Zhou, Weilun Wang, and Houqiang Li. Altfreezing for more general video face forgery detection. In *Proceedings of the IEEE/CVF Conference on Computer Vision and Pattern Recognition*, pages 4129–4138, 2023.
- [89] Haiwei Wu, Jiantao Zhou, and Shile Zhang. Generalizable synthetic image detection via language-guided contrastive learning. *arXiv preprint arXiv:2305.13800*, 2023.
- [90] Yuting Xu, Jian Liang, Gengyun Jia, Ziming Yang, Yanhao Zhang, and Ran He. Tall: Thumbnail layout for deepfake video detection. In *Proceedings of the IEEE/CVF International Conference on Computer Vision*, pages 22658–22668, 2023.
- [91] Zhiyuan Yan, Yong Zhang, Yanbo Fan, and Baoyuan Wu. Ucf: Uncovering common features for generalizable deepfake detection. *arXiv preprint arXiv:2304.13949*, 2023.
- [92] Zhiyuan Yan, Yong Zhang, Xinhang Yuan, Siwei Lyu, and Baoyuan Wu. Deepfakebench: A comprehensive benchmark of deepfake detection. In *Advances in Neural Information Processing Systems*, pages 4534–4565. Curran Associates, Inc., 2023.
- [93] Zhiyuan Yan, Yuhao Luo, Siwei Lyu, Qingshan Liu, and Baoyuan Wu. Transcending forgery specificity with latent space augmentation for generalizable deepfake detection. In *Proceedings of the IEEE/CVF Conference on Computer Vision and Pattern Recognition*, 2024.
- [94] Zhiyuan Yan, Yuhao Luo, Siwei Lyu, Qingshan Liu, and Baoyuan Wu. Transcending forgery specificity with latent space augmentation for generalizable deepfake detection. In *Proceedings of the IEEE/CVF Conference on Computer Vision and Pattern Recognition*, pages 8984–8994, 2024.
- [95] Zhiyuan Yan, Taiping Yao, Shen Chen, Yandan Zhao, Xinghe Fu, Junwei Zhu, Donghao Luo, Li Yuan, Chengjie Wang, Shouhong Ding, et al. Df40: Toward next-generation deepfake detection. *arXiv preprint arXiv:2406.13495*, 2024.
- [96] Xiaohua Zhai, Basil Mustafa, Alexander Kolesnikov, and Lucas Beyer. Sigmoid loss for language image pre-training. In *Proceedings of the IEEE/CVF International Conference on Computer Vision*, pages 11975–11986, 2023.
- [97] Daichi Zhang, Zihao Xiao, Shikun Li, Fanzhao Lin, Jianmin Li, and Shiming Ge. Learning natural consistency representation for face forgery video detection. *arXiv preprint arXiv:2407.10550*, 2024.
- [98] Xu Zhang, Svebor Karaman, and Shih-Fu Chang. Detecting and simulating artifacts in gan fake images. *arXiv preprint arXiv:1907.06515*, 2019.
- [99] Tianchen Zhao, Xiang Xu, Mingze Xu, Hui Ding, Yuanjun Xiong, and Wei Xia. Learning self-consistency for deepfake detection. In *ICCV*, 2021.
- [100] Yinglin Zheng, Jianmin Bao, Dong Chen, Ming Zeng, and Fang Wen. Exploring temporal coherence for more general video face forgery detection. In *ICCV*, pages 15044–15054, 2021.
- [101] Tianfei Zhou, Wenguan Wang, Zhiyuan Liang, and Jianbing Shen. Face forensics in the wild. In *Proceedings of the IEEE/CVF conference on computer vision and pattern recognition*, pages 5778–5788, 2021.
- [102] Jun-Yan Zhu, Taesung Park, Phillip Isola, and Alexei A Efros. Unpaired image-to-image translation using cycle-consistent adversarial networks. In *ICCV*, 2017.
- [103] Mingjian Zhu, Hanting Chen, Qiangyu Yan, Xudong Huang, Guanyu Lin, Wei Li, Zhijun Tu, Hailin Hu, Jie Hu,

and Yunhe Wang. Genimage: A million-scale benchmark for detecting ai-generated image. *Advances in Neural Information Processing Systems*, 36, 2024.

- [104] Xiangyu Zhu, Hao Wang, Hongyan Fei, Zhen Lei, and Stan Z Li. Face forgery detection by 3d decomposition. In *CVPR*, 2021.
- [105] Bojia Zi, Minghao Chang, Jingjing Chen, Xingjun Ma, and Yu-Gang Jiang. Wilddeepfake: A challenging real-world dataset for deepfake detection. In *Proceedings of the 28th ACM international conference on multimedia*, pages 2382–2390, 2020.

Appendix

This appendix material provides additional experimental results, visualizations, and future works:

- Algorithm procedure of the proposed approach (see Sec. A).
- Additional experimental results and ablations (see Sec. B).
- Additional visualizations and analysis (see Sec. D).
- Future works and limitation discussion (see Sec. E).

A. Algorithm Procedure Illustration

Here, we provide an algorithm illustration of the proposed *Effort* approach in Alg. 1 for a comprehensive understanding.

Algorithm 1 *Effort* Approach Algorithm

Input: Pre-trained weight matrix $W \in \mathbb{R}^{n \times n}$; Rank r ; Training data $\mathcal{D} = \{(x_i, y_i)\}_{i=1}^N$; Hyperparameters λ_1, λ_2

Output: Updated weight matrix W

- 1: \triangleright **Step 1: Singular Value Decomposition**
 - 2: Decompose W via SVD: $W = U\Sigma V^\top$
 - 3: Retain top r singular values and vectors:
 - 4: $U_r \in \mathbb{R}^{n \times r}, \Sigma_r \in \mathbb{R}^{r \times r}, V_r \in \mathbb{R}^{n \times r}$
 - 5: Compute $W_r = U_r \Sigma_r V_r^\top$
 - 6: Keep W_r fixed during training
 - 7: Compute residual component: $\Delta W = W - W_r$
 - 8: Decompose ΔW via SVD: $\Delta W = U_{n-r} \Sigma_{n-r} V_{n-r}^\top$
 - 9: Initialize ΔW
 - 10: Define concatenated matrices:
 - 11: $\hat{U} = [U_r, U_{n-r}] \in \mathbb{R}^{n \times n}$
 - 12: $\hat{V} = [V_r, V_{n-r}] \in \mathbb{R}^{n \times n}$
 - 13: \triangleright **Step 2: Training Loop**
 - 14: **for** each epoch **do**
 - 15: **for** each batch in \mathcal{D} **do**
 - 16: \triangleright Forward Pass
 - 17: Compute model output using $W = W_r + \Delta W$
 - 18: Compute classification loss \mathcal{L}_{cls}
 - 19: \triangleright Compute Constraints
 - 20: Compute orthogonality loss:
 - 21: $\mathcal{L}_{\text{orth}} = \left\| \hat{U}^\top \hat{U} - I \right\|_F^2 + \left\| \hat{V}^\top \hat{V} - I \right\|_F^2$
 - 22: Compute singular value constraint loss:
 - 23: $\mathcal{L}_{\text{ksv}} = \left| \left\| \hat{W} \right\|_F^2 - \|W\|_F^2 \right|$
 - 24: \triangleright Total Loss
 - 25: $\mathcal{L} = \mathcal{L}_{\text{cls}} + \lambda_1 \mathcal{L}_{\text{orth}} + \lambda_2 \mathcal{L}_{\text{ksv}}$
 - 26: \triangleright Backward Pass and Optimization
 - 27: Update ΔW using gradient descent to minimize \mathcal{L}
 - 28: **end for**
 - 29: **end for**
 - 30: \triangleright **Step 3: Output**
 - 31: Update the weight matrix: $W \leftarrow W_r + \Delta W$
 - 32: **return** Updated weight matrix W
-

B. Additional Results and Ablations

In this section, we provide additional experimental results and ablation studies to our proposed approach.

B.1. Results on GenImage Benchmark

In our manuscript, we present the benchmarking outcomes of the UniversalFakeDetect Dataset. Additionally, we report the results obtained from another widely utilized benchmark known as GenImage [103]. This GenImage dataset predominantly utilizes the Diffusion model for image generation, incorporating models such as Midjourney [56], SDv1.4 [68], SDv1.5 [68], ADM [18], GLIDE [59], Wukong [1], VQDM [22], and BigGAN [3]. Following the settings defined for GenImage, we designate SDv1.4 as the training set and the remaining models as the test set. Given the diverse image sizes within the GenImage dataset, images with a size smaller than 224 pixels are duplicated and subsequently cropped to 224 pixels, following [79]. We employ the same setting to re-implement FreqNet, FatFormer, and NPR, and also report the results of UnivFD and DRCT from [6].

The results on the GenImage dataset are presented in Table 7. When SDv1.4 is employed as the training set, our method attains an overall accuracy rate of 91.1% across the entire test set. Compared to similar methods that utilize CLIP as the backbone, such as UnivFD and FatFormer, our approach improves accuracy by 11.6% and 2.2%, respectively. Moreover, when contrasted with the latest state-of-the-art (SOTA) method DRCT (ICML 2024), the proposed method achieves a 1.6% enhancement in accuracy. This clearly indicates that our method demonstrates superior generalization capabilities and achieves SOTA performance on the GenImage benchmark.

B.2. Comparison with Existing Video Detectors

In the manuscript, we mainly compare our method with image detectors. Here, we provide an individual result to compare our approach with existing SOTA video detectors. Following [90, 97], we conduct evaluations on the widely-used CDF-v2 [45] and DFDC [15] using the video-level AUC metric. We have considered both the classical detectors such as LipForensics and the latest SOTA detectors such as NACO (ECCV'24) for a comprehensive comparison. Results in Tab. 8 demonstrate that our image-based approach achieves higher generalization performance in both CDF-v2 and DFDC, improving 4.5% and 3.9% points than the second-best video-based models. This further validates the superior generalization performance of our approach.

B.3. Within-Domain Evaluation Results

In the previous contents of the manuscript, we mainly show the cross-domain generalization results. For a more com-

Methods	Venues	Midjourney	SDv1.4	SDv1.5	ADM	GLIDE	Wukong	VQDM	BigGAN	mAcc
ResNet-50 [27]	CVPR 2016	54.9	99.9	99.7	53.5	61.9	98.2	56.6	52.0	72.1
DeiT-S [82]	ICML 2021	55.6	99.9	99.8	49.8	58.1	98.9	56.9	53.5	71.6
Swin-T [49]	ICCV 2021	62.1	99.9	99.8	49.8	67.6	99.1	62.3	57.6	74.8
CNNSpot [86]	CVPR 2020	52.8	96.3	95.9	50.1	39.8	78.6	53.4	46.8	64.2
Spec [98]	WIFS 2019	52.0	99.4	99.2	49.7	49.8	94.8	55.6	49.8	68.8
F3Net [64]	ECCV 2020	50.1	99.9	99.9	49.9	50.0	99.9	49.9	49.9	68.7
GramNet [50]	CVPR 2020	54.2	99.2	99.1	50.3	54.6	98.9	50.8	51.7	69.9
UnivFD [61]	CVPR 2023	91.5	96.4	96.1	58.1	73.4	94.5	67.8	57.7	79.5
NPR [79]	CVPR 2024	81.0	98.2	97.9	76.9	89.8	96.9	84.1	84.2	88.6
FreqNet [78]	AAAI 2024	89.6	98.8	98.6	66.8	86.5	97.3	75.8	81.4	86.8
FatFormer [48]	CVPR 2024	92.7	100.0	99.9	75.9	88.0	99.9	98.8	55.8	88.9
DRCT [6]	ICML 2024	91.5	95.0	94.4	79.4	89.2	94.7	90.0	81.7	89.5
Ours	–	82.4	99.8	99.8	78.7	93.3	97.4	91.7	77.6	91.1

Table 7. **Benchmarking results of cross-method evaluations in terms of Acc performance on the Genimage dataset.** We follow [103] and use the SDv1.4 as the training set while others as the testing sets. We directly cite the results of ResNet-50, DeiT-S, Swin-T, CNNSpot, Spec, F3Net, and GramNet from [103]. We obtain the results of UnivFD and DRCT from [6], and FreqNet, NPR, and FatFormer by using the official checkpoints for reproduction. We report the Accuracy metric for comparison following [6].

Methods	Venues	CDF-v2	DFDC	Avg.
LipForensics [25]	CVPR 2021	0.824	0.735	0.780
FTCN [100]	ICCV 2021	0.869	0.740	0.805
HCIL [23]	ECCV 2022	0.790	0.692	0.741
RealForensics [26]	CVPR 2022	0.857	0.759	0.808
LTTD [24]	NeurIPS 2022	0.893	0.804	0.849
AltFreezing [88]	CVPR 2023	0.895	–	–
TALL-Swin [90]	ICCV 2023	0.908	0.768	0.838
StyleDFD [12]	CVPR 2024	0.890	–	–
NACO [97]	ECCV 2024	0.895	0.767	0.831
Ours	–	0.956	0.843	0.900

Table 8. **Cross-dataset generalization evaluations with existing SOTA video detectors.** The results of other detectors are directly cited from their original papers. The metric is video-level AUC.

Methods	CDF-v2	DFD	DFDC	Avg.
LoRA [37]	0.838	0.834	0.717	0.796
MoE-LoRA [38]	0.867	0.904	–	–
Dual-Adapter [71]	0.717	–	0.727	–
Ours	0.901	0.923	0.798	0.874

Table 9. **Cross-dataset generalization evaluations with other adapter-based partially fine-tuned detectors.** The results are cited from their original papers. The metric is **frame-level AUC**.

prehensive evaluation, we provide our method’s within-domain evaluations. Since we use FF++ [70] (c23) for training, following DeepfakeBench [92], we train our model on FF++ (c23) and test it on FF++ (c23) and FF++ (c40), where c40 is a compression version of c23. We compare the re-

Archs.		$n - r$	r	mAcc
UniFD [61] (Linear-Prob)		–	–	81.02
Baseline (FFT)		–	–	86.22
Ours	Variant-1	256	–	92.13
	Variant-2	64	–	93.68
	Variant-3	16	–	94.45
	Variant-4	4	–	94.37
	Variant-5	1	–	95.19
LoRA	Variant-1	–	256	91.42
	Variant-2	–	64	91.06
	Variant-3	–	16	91.89
	Variant-4	–	4	93.53
	Variant-5	–	1	93.03

Table 10. **Ablation studies on synthetic image detection (UniversalFakeDetect Dataset) regarding the tunable $n - r$ values in SVD (Ours) and r values in LoRA.** All models are trained on ProGAN’s images and tested on 19 different kinds of generative models’ images. “FFT” indicates the full fine-tuning. “Linear-Prob” indicates fine-tuning FC layer only, where we reproduce the results from UniFD [61].

sults of our approach with other competing baseline models such as CNN-Aug, F3Net, SPSL, SRM, and RECCE from DeepfakeBench. We also compare our approach with the latest SOTA detector, *i.e.*, CDFA [46] (ECCV’24) for a comprehensive comparison. Results in Tab. 11 show that generally, all detectors perform very well on FF++ (c23), as the training and testing distributions are similar. However, the performance largely drops when applying compression (tested on the c40 version). Also, our approach demonstrates the best results on FF++ (c40), showing the robustness of our detector. Notably, it can be seen that although CDFA achieves superior generalization results on cross-domain evaluation scenarios, it’s performance on within-domain evaluation is limited. In contrast, our approach

shows high results on both within-domain and cross-domain evaluations. Regarding the model’s robustness toward the post-processing, we provide another robustness experiment following [32] (refer to Sec. B.5 for details).

B.4. Comparison with Existing Adapter-Based Detectors

Parameter-efficient fine-tuning (PEFT) has become a popular technique for adapting pre-trained vision foundation models (VFM) to downstream tasks. Low-ranked adaptation (LoRA) [29] is a widely-used approach for PEFT. Previous works [37, 48] employing LoRA in the VFMs have achieved good empirical generalization results on both deepfake detection and synthetic image detection benchmarks. Compared to full parameter fine-tuning (FFT), LoRA also has the advantage of retaining part of the original well-learned pre-trained semantic knowledge while learning the forgery patterns. Additionally, [38] and [71] introduce MoE-LoRA techniques and dual adapters into the deepfake detection fields. However, our SVD-based approach differs from these adapter-based methods and shows several advantages over them. Specifically, our method **explicitly** constructs two **orthogonal subspaces** for semantic and forgery using SVD, ensuring the pre-existing semantic knowledge will not be distorted and well-retained during the process of learning forgery. In contrast, the mentioned adapter-based methods do not explicitly ensure the orthogonality between semantic and forgery, still having the potential to distort the pre-existing semantic knowledge and result in unexpected generalization results.

To show our approach can achieve better generalization results than other adapter-based methods in both deepfake detection and synthetic image detection benchmarks, we provide several empirical results in Tab. 9 and Tab. 10. From these results, we can see that our proposed SVD-based method achieves clearly higher generalization results than adapter-based methods in both deepfake detection and synthetic image detection fields, as our approach explicitly preserves the semantic knowledge while learning the forgery patterns.

B.5. Robustness Evaluation

To evaluate our model’s robustness to random perturbations, we adopt the methodology used in previous studies [25, 100], which involves examining three distinct types of degradation: Block-wise distortion, Change contrast, and JPEG compression. We apply each of these perturbations at five different levels to assess the model’s robustness under varying degrees of distortion, following [9, 93]. The video-level AUC results for these unseen perturbations, using the model trained on FF++ (c23), are depicted in Fig. 8. Generally, our approach shows higher results than other methods, demonstrating the better robustness of our approach than

Methods	FF-c23	FF-c40	Avg.
CNN-Aug [86]	0.8493	0.7846	0.8170
F3Net [64]	0.9635	0.8271	0.8953
SPSL [47]	0.9610	0.8174	0.8892
SRM [53]	0.9576	0.8114	0.8845
RECCE [4]	0.9621	0.8190	0.8906
CDFAT† [46]	0.9025	0.6938	0.7982
Ours	0.9872	0.8429	0.9151

Table 11. **Within-domain evaluations using the video-level AUC metric.** All detectors are trained on FF-c23 and evaluated on other data. † donates our reproduction using the pre-trained weights, otherwise, we obtain the results from [92].

Methods	GID-DF		GID-F2F	
	Acc	AUC	Acc	AUC
EfficientNet [80]	82.40	91.11	63.32	80.10
MLGD [41]	84.21	91.82	63.46	77.10
LTW [74]	85.60	92.70	65.60	80.20
DCL [75]	87.70	94.90	68.40	82.93
M2TR [84]	81.07	94.91	55.71	76.99
F3Net [64]	83.57	94.95	61.07	81.20
F2Trans [55]	89.64	97.47	81.43	90.55
CFM [52]	85.00	92.74	76.07	84.55
FA-ViT [51]	92.86	98.10	82.57	91.20
Ours	95.71	99.26	85.71	93.83

Table 12. **Additional results of cross-manipulation evaluation on FF++ (c23).** Following [51, 55], we conduct evaluations by training on the other three manipulated methods while testing on the remaining one. Specifically, GID-DF means training on the other three manipulated methods (FF-F2F, FF-FS, FF-NT) while testing on the FF-DF. Results of other methods are cited from [51, 55].

other models.

C. Additional cross-method evaluation

The capability of face forgery detectors to generalize to new manipulation methods is crucial in practical, real-world applications. In our manuscript, we present cross-method evaluations using the DF40 dataset [95]. Specifically, we train the models with four manipulation methods from FF++ (c23) and then test them on the other eight manipulation techniques provided in DF40. Furthermore, we conduct an additional cross-method evaluation following the protocol introduced in [51, 55, 75]. This protocol involves training the model on diverse manipulation types of samples and subsequently testing it on unknown manipulation methods. The results of this evaluation are reported in Tab. 12. It is evident that our proposed method attains remarkable performance in cross-manipulation evaluation. In terms of accuracy (ACC), it outperforms the latest SOTA detector FA-ViT by 2.85% on GID-DF and 3.14% on GID-

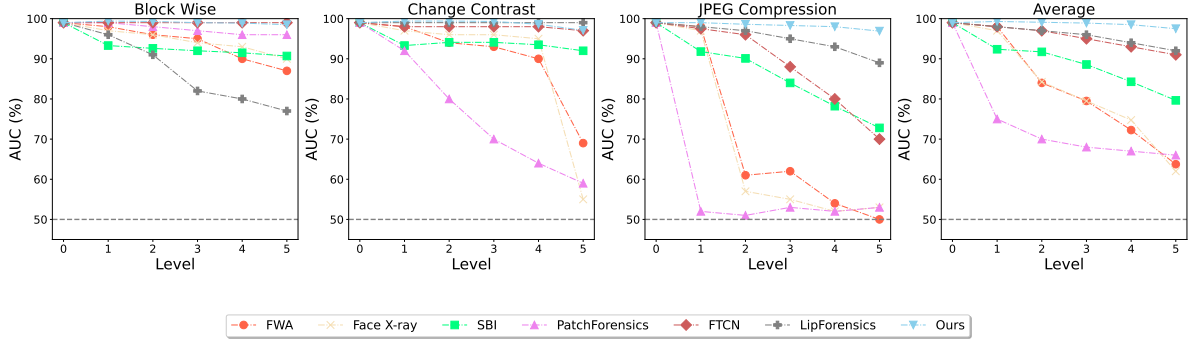


Figure 8. **Robustness to unseen perturbations.** We present video-level AUC for five distinct degradation levels across three types of perturbations in [32].

VFMs	#Params	#ImgSize	CDF-v2	SimSwap	Avg.
BEIT-v2 [63]	303M	224	0.855	0.821	0.838
+ Ours	0.14M	224	0.894	0.850	0.872
SigLIP [96]	316M	256	0.877	0.713	0.795
+ Ours	0.19M	256	0.895	0.778	0.867
CLIP [65]	307M	224	0.857	0.860	0.859
+ Ours	0.19M	224	0.956	0.926	0.941

Table 13. **Ablation studies on deepfake image detection (Cross-dataset) regarding different vision foundation models (VFMs) were used.** All models are trained on FF++ (c23) and tested on CDF-v2 and SimSwap.

VFMs	#Params	#ImgSize	mAP	mAcc
BEIT-v2 [63]	303M	224	93.50	79.11
+ Ours	0.14M	224	97.39	83.66
SigLIP [96]	316M	256	94.30	81.23
+ Ours	0.19M	256	96.24	90.46
CLIP [65]	307M	224	97.95	86.22
+ Ours	0.19M	224	99.41	95.19

Table 14. **Ablation studies on synthetic image detection (UniversalFakeDetect Dataset) regarding different vision foundation models (VFMs) were used.** All models are trained on ProGAN’s images and tested on 19 different generative models’ images.

F2F, respectively.

C.1. Additional Ablation Studies

Impact of Different Vision Foundation Models We initialize the ViT backbone with several widely used pre-trained weights from different vision foundation models, including BEIT-v2 [63], CLIP [65], and SigLIP [96]. The results are shown in Tab. 13 and Tab. 14. It is evident that our proposed approach improves the generalization performance of different pre-trained ViTs. On the other hand, we note that different initialization significantly impacts generalization performance, indicating the importance of choos-

VFMs	#Params	#ImgSize	CDF-v2	SimSwap	Avg.
CLIP-Base/16	86M	224	0.854	0.833	0.844
+ Ours	0.07M	224	0.915	0.919	0.917
CLIP-Large/14	307M	224	0.857	0.860	0.859
+ Ours	0.19M	224	0.956	0.926	0.941

Table 15. **Ablation studies on deepfake image detection (Cross-dataset) regarding different ViT architectures were used.** We employ the two architectures implemented in the original paper of CLIP [65] for experiments. All models are trained on FF++ (c23).

VFMs	#Params	#ImgSize	mAP	mAcc
CLIP-Base/16	86M	224	96.25	82.52
+ Ours	0.07M	224	98.47	88.46
CLIP-Large/14	307M	224	97.95	86.22
+ Ours	0.19M	224	99.41	95.19

Table 16. **Ablation studies on synthetic image detection (UniversalFakeDetect Dataset) regarding different architectures were used.** All models are trained on ProGAN’s images and tested on 19 different kinds of generative models’ images.

ing a suitable pre-trained initialization. Through empirical results, we discover that the ViT pre-trained on CLIP exhibits the highest performance in both deepfake detection and synthetic image detection tasks. Therefore, we choose CLIP as the default setting for our approach.

Impact of Different ViT Backbones Here, we investigate the effects of different ViT architectures. Specifically, we consider two backbones that were implemented in the original paper of CLIP: ViT-Base-16 and ViT-Large-14. We conduct evaluations on both deepfake detection and synthetic image detection benchmarks, as shown in Tab. 15 and Tab. 16. Compared to fully fine-tuning the CLIP model, our proposed approach consistently demonstrates substantial enhancements in generalization performance across these ViT backbones. It is worth noting that CLIP-Large performs better than CLIP-Base by a notable

(a). Vanilla CNN



(a). Ours

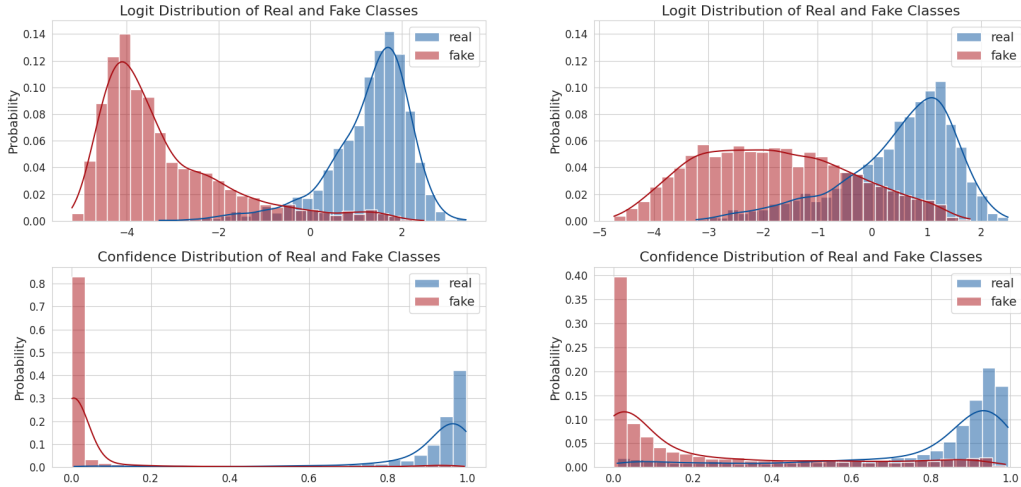


Figure 9. **Logits and confidence distributions of the vanilla CNN (Xception) and ours.** We show that (a) the Xception fits the fake patterns in the training set well (the left column), while other information is not adequately captured, leading to poor generalization when detecting unseen deepfake datasets (the right column). In contrast, our approach (b) learns both forgery patterns and semantic knowledge well, achieving more robust generalization performance.

margin. Based on this ablation experiment, we ultimately choose ViT-Large as our default backbone.

D. Additional Analysis and Visualizations

D.1. Logit Distribution Analysis

We show the prediction distribution of a naive trained detector’s output (real probabilities) in Fig. 9. We see that the vanilla CNN detector tends to learn the fake in the training set and cannot learn a good feature of real when evaluating unseen fakes. When the fake patterns are unseen during

training, the logit for real/fake classification tends to be very unconfident. Additionally, the overlapping between real and fake classes of Xception is significantly increased when detecting unseen the forgery dataset. In contrast, our approach preserves semantic knowledge while learning forgery patterns during training, thereby improving the model’s generalization performance.

D.2. Additional t-SNE Visualizations

In our manuscript, we visualize the t-SNE of the seen fake ProGAN and unseen fake StyleGAN for the comparison of

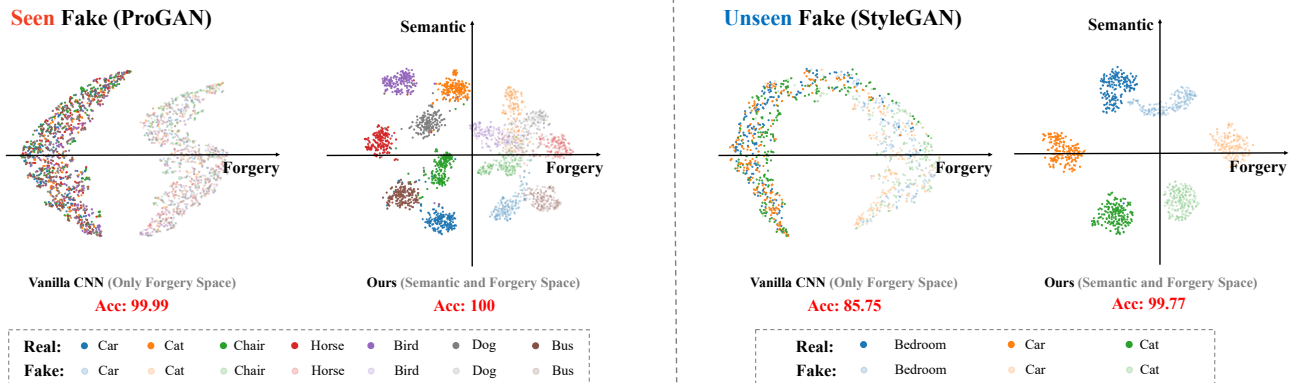


Figure 10. **t-SNE visualizations of the latent feature spaces between vanilla CNN [86] and ours.** We use the testing set of ProGAN and StyleGAN within UniversalFakeDetect Dataset [86] for visualization.

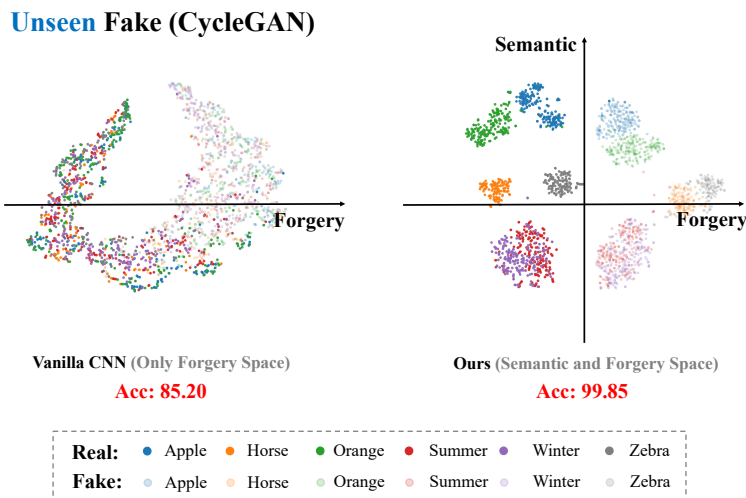


Figure 11. **t-SNE visualizations of the latent feature spaces between vanilla CNN [86] and ours.** We use the testing set of CycleGAN within UniversalFakeDetect Dataset [86] for visualization.

vanilla CNN (Res-50 [86]) and ours (see Fig. 10). Now, we provide additional t-SNE visualizations, including t-SNE results between vanilla CNN and ours on **CycleGAN**, as shown in Fig. 11. As we can see from both two figures, our approach maximizes and preserves the semantic knowledge while fitting the forgery patterns during training, whereas the vanilla CNN overfits the seen fake method, learning forgery patterns only, thereby resulting in a highly low-ranked feature space (see Fig. 6 and Fig. 7 of the manuscript for details) and causing the overfitting to seen forgery patterns in the training set. Additionally, we see that the logit distribution of the vanilla CNN has a larger overlapping between fake and real, while ours is highly smaller, suggesting that our approach achieves a better generalization performance.

E. Limitation and Future Work

The core idea of this paper is to decompose the original semantic space into two orthogonal subspaces for preserving semantic knowledge while learning the forgery. In our manuscript and appendix, we have conducted extensive experiments and in-depth analysis on both deepfake and synthetic image detection benchmarks, showing the superior advantages in both generalization and efficiency. One limitation of our work is that our approach regards all fake methods in one class during training real/fake classifiers, potentially ignoring the specificity and generality of different fake methods.

In the future, we plan to expand our approach into a *incremental learning* framework, where each fake method will be regarded as “one SVD branch”, ensuring the orthogonality between different fake methods, thereby avoiding the severe forgetting of previous learned fake methods. This extension design will help our approach better address the

future deepfake types in the real-world scenario. Additionally, although our work's scope mainly focuses on deepfake and synthetic image detection, our approach also has the potential to be applied to other similar fields such as face anti-spoofing, anomaly detection, etc. Furthermore, we hope our proposed approach can inspire future research in developing better orthogonal modeling strategies.

Ethics & Reproducibility. All of the facial images that are utilized are sourced from publicly available datasets and are accompanied by appropriate citations. This guarantees that there is no infringement upon personal privacy. We will make all codes and checkpoints available for public access upon acceptance.